Macromolecules

ARTICLE

pubs.acs.org/Macromolecules

Circularly Polarized Light Enhancement by Helical Polysilane Aggregates Suspension in Organic Optofluids

Yoko Nakano[§] and Michiya Fujiki*

Graduate School of Materials Science, Nara Institute of Science and Technology (NAIST), 8916-5 Takayama, Ikoma, Nara 630-0192, Japan

Supporting Information

ABSTRACT: Circularly polarized (CP) light may play key roles in the migration and delocalization of photoexcited energy in optically active macroscopic aggregates of chiral chlorophylls surrounded by an aqueous fluid in the chloroplasts under incoherent unpolarized sunlight. Learning from the chiral fluid biosystem, we designed artificial polymer aggregates of three highly luminescent helical polysilanes, **1-*S***, **2-*S***, and **2-*R*** (Chart 1). Under specific conditions (molecular weights and good-and-poor solvent ratio), **1-*S*** aggregates with ~5 μm in organic fluid generated an efficient circularly polarized luminescence (CPL) with $g_{CPL} = -0.7$ at 330 nm while retaining a high quantum efficiency (Φ_{PL}) ~53% at room temperature under incoherent unpolarized photoexcitation at 290 nm. This huge g_{CPL} value was the consequence of the intense bisignate circularly dichroism (CD) signals ($g_{CD} = -0.35$ at 325 nm and +0.31 at 313 nm) due to coupled oscillators with electric-dipole-allowed-transition origin. Also, **2-*S*** and **2-*R*** aggregates gave almost identical intense CD and CPL amplitudes of **1-*S***. The most critical factors for the CD/CPL enhancements were the molecular weights of **1-*S***, **2-*S***, and **2-*R*** and a refractive index of good/poor cosolvents. The former was connected to a long persistence length of ~70 nm, characteristic of rod-like helical polysilanes. The latter was due to an efficient photoexcited energy confinement effect of slow CP-light in the aggregate.

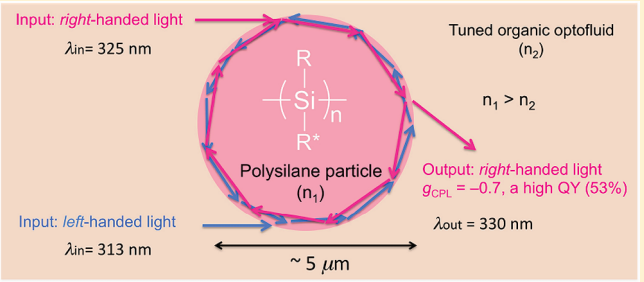

INTRODUCTION

Circularly polarized (CP) light may play key roles in the migration and delocalization of photoexcited energy in optically active macro-aggregates containing ~10^8 chlorophylls under incoherent unpolarized sunlight.[1,2] This aggregation behavior requires the presence of three chiral centers at the periphery of the chlorophylls and two chiral centers in the long alkyl tail of the chlorophylls. Because these chiral aggregates are surrounded by an aqueous fluid (stroma) in the chloroplasts, the CP light-related photophysical properties are susceptible to changes in osmotic pressure, Mg^{2+}/K^+ ions, sunlight intensity, and temperature.[2] Although the relationship between the chiral aggregates and the stroma is not well understood, this fluid chiral biosystem led us to design artificial, chiral supramolecular polymer aggregates dispersed in an organic fluid. This system is composed of a highly luminescent helical rod polymer consisting of an Si−Si main chain and chiral side chains[3,4] (polysilanes **1-*S***, **2-*S***, and **2-*R***, Chart 1 and Scheme S1 in Supporting Information) dispersed in a mixture of two organic solvents. Herein, we show that under optimized conditions, **1-*S*** aggregates (average size, ~5 μm) in the suspension can very efficiently generate circularly polarized luminescence (CPL) with $g_{CPL} = -0.7$ and a narrow, full-width-half-maximum (*fwhm*) of 0.18 eV (1450 cm^{-1}) while retaining a high Φ_{PL} (~53% at 330 nm, 3.75 eV) at room temperature under incoherent unpolarized photoexcitation at 290 nm. This huge g_{CPL} value results from the intense bisignate circular dichroism (CD) signals ($g_{CD} = -0.35$ at 325 nm (3.82 eV) and +0.31 at 313 nm (3.96 eV)) that arise from collective coupled oscillators with electric-dipole-allowed-transition (*edat*) origins.

Chart 1. Chemical Structures of Poly{*n*-decyl-(*S*)-2-methylbutylsilane} (1-*S*), Poly{*n*- dodecyl-(*S*)-2-methylbutylsilane} (2-*S*), and Poly{*n*-dodecyl-(*R*)-2-methylbutylsilane} (2-*R*)

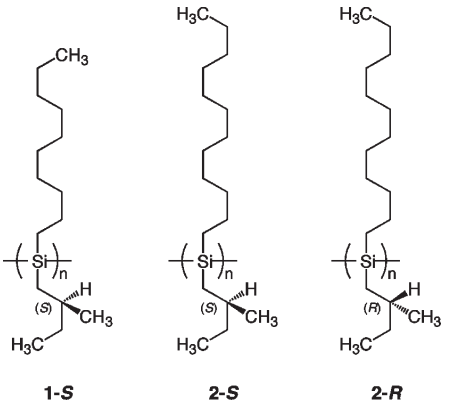

Received: July 20, 2011
Revised: August 27, 2011
Published: September 16, 2011

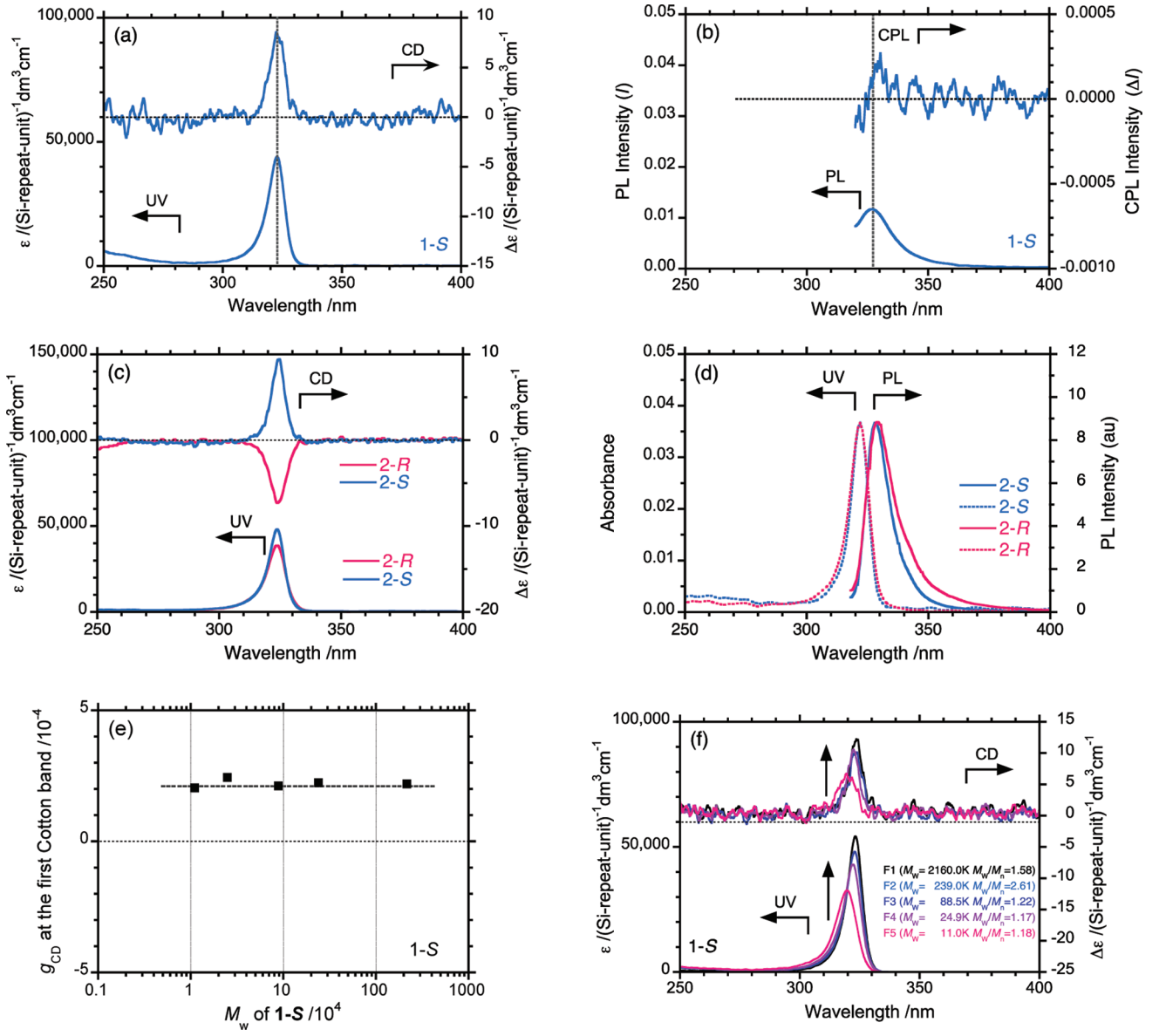

Figure 1. (a) Typical CD and UV spectra at 25.0 °C ([Si repeating unit] = 1.25×10^{-5} mol L^{-1}) and (b) CPL and PL spectra excited at 290 nm at room temperature (26.4 °C) ([Si repeating unit] = 1.25×10^{-6} mol L^{-1}) of **1-*S*** (M_w = 88 500, M_w/M_n = 1.22) dispersed molecularly in THF. (c) Typical CD and UV and (d) UV and PL spectra of **2-*S*** (blue lines, M_w = 108 000, M_w/M_n = 2.89) and **2-*R*** (red lines, M_w = 80 900, M_w/M_n = 2.34) dissolved molecularly in isooctane at 25.0 °C. [Si repeating unit] = 2.0×10^{-6} mol L^{-1}. (e) The values of g_{CD} at ~323 nm for **1-*S*** at 25.0 °C as a function of molecular weight (M_w). (f) CD and UV spectra of **1-*S*** with five different molecular weights (Table S1, Supporting Information) in THF at 25.0 °C.

RESULTS AND DISCUSSION

Recently we reported that several optically active π-conjugated polymer aggregates (averaged size of several μm) dispersed in organic fluid solutions exhibit fairly efficient CPL ($|g_{CPL}|$ = 0.06−0.07 at 510−530 nm) upon incoherent *unpolarized* photoexcitation in association with a high $|g_{CD}|$ ~0.08 at 510 nm; however, surprisingly, Φ_{PL} remained as high as 84−91% based on *edat* origins.[5] This finding contrasts with the explanation in classical textbooks, which states that aggregates of aromatic hydrocarbons generally quench their fluorescence due to formation of sandwich-shaped $\pi-\pi$ stacks, leading to significant suppression of long-range energy migration.[6] However, recent studies have demonstrated that aggregate forms of aromatic compounds and hyperbranched polymers dispersed in solvents do not experience suppression of their inherent fluorescence when appropriate substituents are introduced.[7]

CD/CPL active aggregates have been generated by photoluminescent, nonhelical π-conjugated polyfluorene derivatives with the aid of the (*S*)- and (*R*)-limonene chirality transfer.[5] The solution required a mixture of three solvents: a good solvent to dissolve the polymers, a poor solvent to precipitate the polymers, and a chiral solvent (terpenes) to induce chirality in the achiral polymers. Although the $|g_{CD}|$ and $|g_{CPL}|$ values were maximized at a very specific volume fraction of these tersolvents,[5] the essential role of these solutions remained unclear; the mixed solvent may simply act as dispersion media or have other functions.

Knowledge and understanding from the realm of condensed matter physics and quantum physics are now applicable to soft

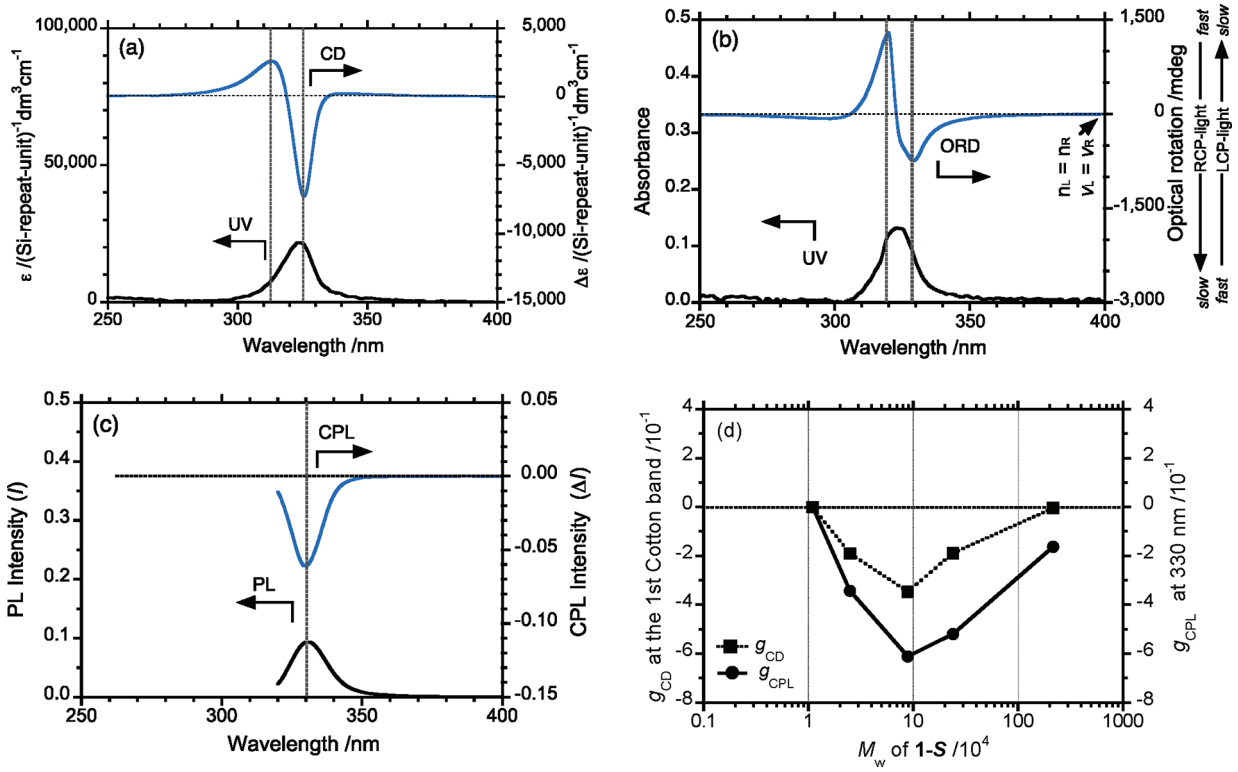

Figure 2. (a) CD and UV spectra (25.0 °C), (b) ORD and UV spectra (25.0 °C) and (c) CPL and PL spectra (26.4 °C) excited at 290 nm of **1-*S*** (M_w = 88 500, M_w/M_n = 1.22) aggregates formed in THF/methanol (1.7/1.3 (v/v)) using an 800 rpm (CW) stir rate for (a, b) ([Si repeating unit] = 6.25 × 10^{-6} mol L^{-1}). (d) Values of g_{CD} (dotted line with filled squares) at 325 nm for **1-*S*** in THF/methanol (1.7/1.3 (v/v)) at 25.0 °C with an 800 rpm (CW) stir rate and values of g_{CPL} (solid line with filled circles) at 330 nm for **1-*S*** in THF/methanol (1.7/1.3 (v/v)) at room temperature (23.5 °C) without stirring as a function of the molecular weight (M_w) of **1-*S***. [Si repeating unit] = 6.25 × 10^{-6} mol L^{-1}.

matters, including biosystems and artificial systems. For example, two-dimensional photon-echo (2DPE) spectroscopy has revealed that, in biological photosynthetic systems, including green sulfur bacteria and marine algae dispersed in aqueous solutions, quantum coherence and/or quantum beating are occurring, enabling efficient energy transfer between plural chromophores positioned over a long distance at cryogenic and even ambient temperatures.[8,9] These 2DPE spectroscopy and anisotropy decay experiments revealed that even the very typical π-conjugated polymer (poly[2-methoxy-5-(2′-ethylhexoxy)-1,4-phenylenevinylene], (MEH-PPV) dissolved in a good solvent,[10] and the quantum coherence in the electronic and vibrational transitions occurred at room temperature.[11] Recently, an increasing amount of attention has been focused on slow-light phenomena as well as the fundamentals and applications, such as laboratories-on-a-chip, of light-matter interactions in electromagnetically strongly dispersive environments.[12,13] Slow-light refers to the propagation of an optically input pulse or other modulation of an optical carrier at a low group velocity. The term is usually applied to when the velocity is at least hundreds of times slower than the speed of light in a vacuum.[13] However, optical rotatory dispersion (ORD) spectroscopy allows us to sensitively detect a subtle difference in the velocity of left- and right-CP light of the matter dispersed in an isotropic media.[14]

Theoretical studies have shown that greatly enhanced CD signals are possible in the Bragg stacks composed of a nonchromophoric polymer dispersed in chiral organic media as well as in a chirally sculptured thin film infiltrated with achiral organic fluid.[12]

Our successful results with the optically active π-conjugated polymer aggregates prompted us to study optically active aggregates consisting of helical σ-conjugated polysilanes, poly[*n*-decyl-(*S*)-2-methylbutylsilane] (**1-*S***), poly[*n*-dodecyl-(*S*)-2-methylbutylsilane] (**2-*S***), and poly[*n*-dodecyl-(*R*)-2-methylbutylsilane] (**2-*R***) (Chart 1) surrounded by achiral organic fluid. The persistence length (q), a measure of chain stiffness, of **1-*S*** reaches up to 70 nm in fluid solution at room temperature.[4,15] These polysilanes can adopt an ideal rod structure up to the degree of polymerization (DP) ~400, corresponding to a weight-averaged polymer molecular weight (M_w) ~72 000 at ambient temperature. The former characteristic is in sharp contrast to typical polymers,[4,15,16] *e.g.*, poly(*n*-hexyl isocyanate) (q = 20−43 nm), poly(dialkylfluorene) (q = 7−9 nm), and double-stranded DNA (q = 60 nm).[15]

The most striking feature of the helical rod polysilanes **1-*S***, **2-*S***, and **2-*R*** molecularly dissolved in dilute tetrahydrofuran (THF) is that they exhibit uniquely intense, narrow absorption, CD and photoluminescence (PL) bands featuring *fwhm* of ~0.10 eV (~800 cm^{-1}), no phonon-side-bands, and a very small Stokes shift of ~0.05 eV (~400 cm^{-1}) (Figures 1a−1f and Table S1 (Supporting Information)).[3,4] The absence of phonon-side bands is due to inefficient electron−phonon coupling arising from a low-energy stretching vibration mode of the heavier Si−Si bonds (~500 cm^{-1}, 0.06 eV). These photophysical properties reflect ideal one-dimensional helical exciton characteristics in a fluid solution at room temperature.[3,4] Thus, an efficient optical confinement into a quantum wire with 0.2 nm silicon wire-width surrounded by long alkyl side chains (~2 nm in length) is realized.[3,4,16] An exciton binding energy of ~1 eV is sufficiently high to result in a very thermally stable exciton state with a very fast PL decay of 100−200 psec.[4,17] However, the $|g_{CD}|$ value for

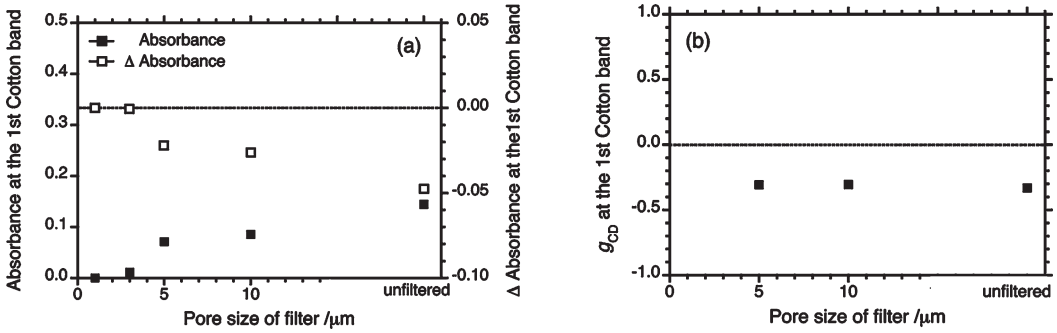

Figure 3. (a) Changes in CD and UV intensities at 325 nm and (b) changes in the g_{CD} values for **1-*S*** (M_w = 88 500, M_w/M_n = 1.22) aggregates formed in THF/methanol (1.7/1.3 (v/v)) at 25 °C, using an 800 rpm (CW) stir rate as a function of membrane filter pore size. [Si repeating unit] = 6.25 × 10^{-6} mol L^{-1}.

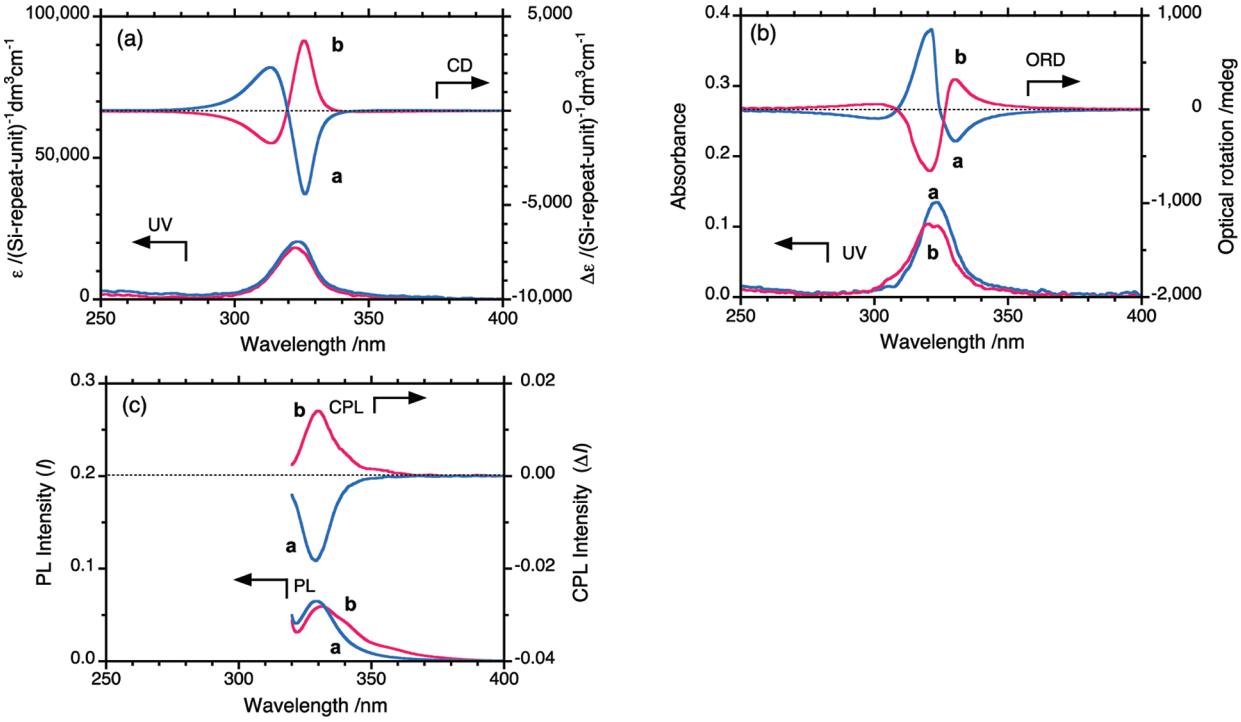

Figure 4. (a) CD/UV, (b) ORD/UV, and (c) CPL/PL spectra excited at 290 nm for **2-*S*** (a; blue line; M_w = 108 000, M_w/M_n = 2.89) and **2-*R*** (b; red line; M_w = 80 900, M_w/M_n = 2.34) aggregates formed in THF/methanol (1.3/1.7 (v/v)) at room temperature. [Si repeating unit] = 6.25 × 10^{-6} mol L^{-1}. CD/UV and ORD/UV spectra were recorded at 25.0 °C using an 800 rpm (CW) stir rate.

1-*S*, **2-*S*** and **2-*R*** molecularly dispersed in THF is only ~2 × 10^{-4}. This weakness is inherent in the 7_3 helical polysilane main chain,[3,4] corresponding to a dihedral angle (θ) of ~155° with right-handed-screw-sense (P) and θ ~205° with left-handed-screw-sense (M) in the ground state.[3,4] The value of g_{CD} does not depend on the M_w of **1-*S*** in solutions because there is a loss of main chain mobility (Figure 1e). However, the expected CPL signal, $|g_{CPL}|$ ~2 × 10^{-4}, cannot be clearly observed, possibly due to a loss of helix preference in the excited state and/or limitations in our CPL instrument sensitivity (Figure 1b).

Conversely, the polysilane aggregates dispersed in organic media exhibited very enhanced Cotton CD, ORD, and CPL signals. Parts a−c of Figure 2 display typical CD/UV, ORD/UV, and CPL/PL spectra of **1-*S*** (M_w = 88 500, polydispersity index (PDI) = 1.22) aggregates using the optimized volume fraction of THF/methanol (1.7/1.3 (v/v)) and the optimized M_w value (Figure S2 (Supporting Information)). The averaged aggregate size was ~5 μm based on membrane filtration experiments using various pore sizes (Figures 3 and S1 (Supporting Information)). The CD spectrum in the main chain $\sigma-\sigma^*$ transition region exhibited a bisignate Cotton effect with a large amplitude containing both positive and negative signals.[15,16] This signal is a consequence of what is known as the coupled-oscillator of the lowest excitonic Siσ−Siσ^* transitions among the nearest neighbor chromophores.[4,18] The bisignate CD profile of **2-*S*** is almost identical to that of **1-*S*** (Figures 2a, 4a, S3b, and S5b (Supporting Information)); conversely, the opposite profile is observed for **2-*R*** (Figures 4a, S3a, and S5a (Supporting Information)). The g_{CD} amplitudes of −0.35 (**1-*S***), −0.22 (**2-*S***), and +0.23 (**2-*R***) were obtained at the first Cotton band around 325 nm (Figures 2a and 4a). The CPL and PL spectra of **1-*S*** aggregates show a pronounced Cotton signal located at ~330 nm (Figures 2c, 5b, and S2b (Supporting Information)). The magnitude of the g_{CPL} value reaches as high as −0.70 at ~330 nm under *unpolarized* excitation at 290 nm.

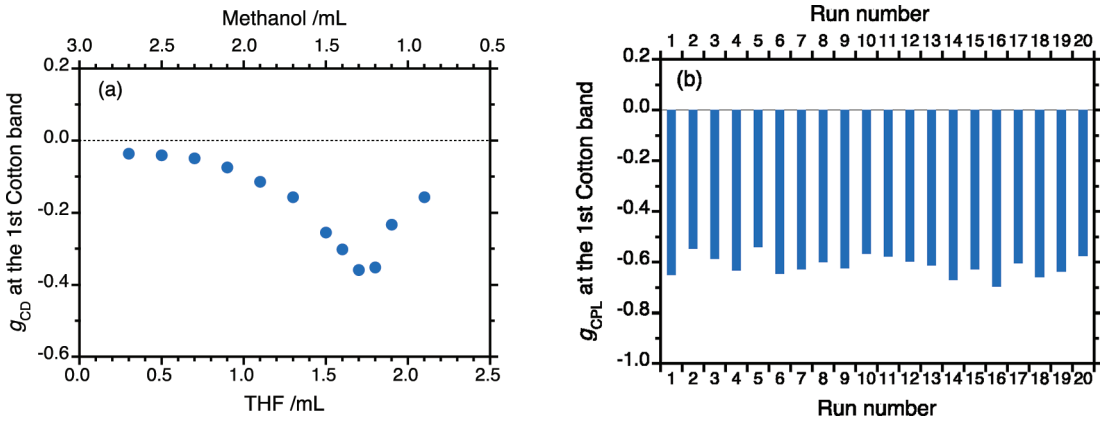

Figure 5. (a) Values of g_{CD} at ~325 nm for **1-*S*** (blue circles; M_w = 88 500, M_w/M_n = 1.22) in THF/methanol at 25 °C, using an 800 rpm (CW) stir rate, as a function of THF/methanol volume fraction. [Si repeating unit] = 6.25 × 10^{-6} mol L^{-1}. (b) g_{CPL} values at 330 nm for 20 independent samples of **1-*S*** aggregates (blue bars) in THF/methanol (1.7/1.3 (v/v)) at room temperature (25.9 °C). [Si repeating unit] = 6.25 × 10^{-6} mol L^{-1}.

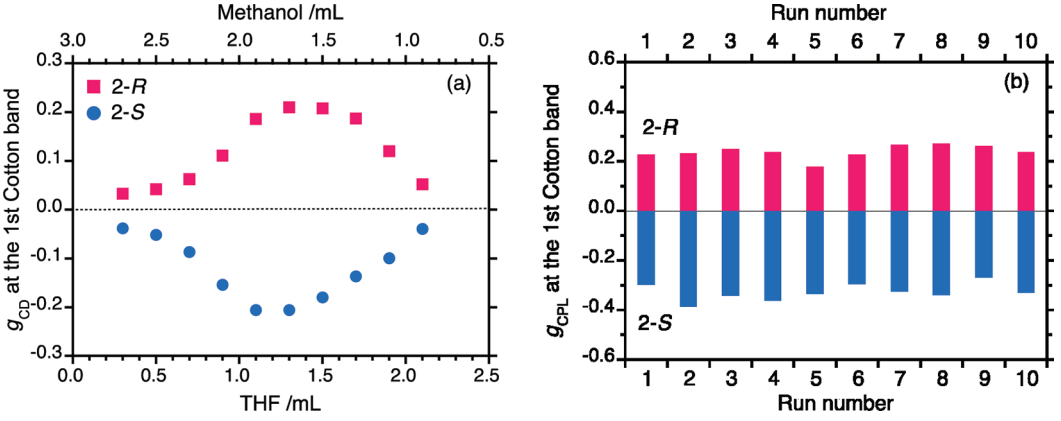

Figure 6. (a) Values of g_{CD} at ~325 nm for **2-*R*** (red squares; M_w = 80 900, M_w/M_n = 2.34) and **2-*S*** (blue circles; M_w = 108 000, M_w/M_n = 2.89) in THF/methanol at 25.0 °C, using an 800 rpm (CW) stir rate, as a function of THF/methanol volume fraction. [Si repeating unit] = 6.25 × 10^{-6} mol L^{-1}. (b) g_{CPL} values at 330 nm for ten independent samples of **2-*R*** (red bars; M_w = 80 900, M_w/M_n = 2.34) and **2-*S*** (blue bars; M_w = 108 000, M_w/M_n = 2.89) aggregates in THF/methanol (1.3/1.7 (v/v)) at room temperature (25.9 °C). [Si repeating unit] = 6.25 × 10^{-6} mol L^{-1}.

Moreover, **1-*S*** aggregates retain a very high Φ_{PL} value of 0.53, which was determined relative to a Φ_{PL} of 0.76 for poly(methyl-*n*-propylsilane) as a reference.[17] Similarly, the **2-*S*** and **2-*R*** aggregates under optimized THF/methanol conditions and M_w showed pronounced CPL at ~330 nm (Figures 4c and 6b, S3, and S5 (Supporting Information)). The magnitudes of g_{CPL} at 330 nm under steady state excitation at ~290 nm are −0.27 (**2-*S***) and +0.23 (**2-*R***) (Figures 4c, 6b, and S3 (Supporting Information)). The presence of *n*-alkyl side chains allows for arrangement of the polysilane chains into a nearest-neighbor separation of ~2 nm in the aggregate form,[16] which may allow the high Φ_{PL} value inherent to polysilanes to be retained and prevent PL quenching.

For conventional chiral molecules and polymers in isotropic media,[18,19] the degree of g_{CD} and g_{CPL} are determined with g = 4 $|\boldsymbol{m}|$ $|\boldsymbol{\mu}|$ cosθ ($|\boldsymbol{m}|^2$ + $|\boldsymbol{\mu}|^2$)$^{-1}$ where θ is the angle between the magnetic and electric dipole transition moments $\boldsymbol{m}$ and $\boldsymbol{\mu}$. The magnitude of $\boldsymbol{\mu}$ is typically of an order of 1 μ_D (Debye) ~10^{-18} esu, while the magnitude of $\boldsymbol{m}$ is an order of 1 μ_B (Bohr magnetron) ~10^{-20} emu. Therefore, similar to isolated chiral molecules and helical polymers in isotropic media, when they arise primarily from *edat* origins, intense absorption and emission bands are observed,[19] and the absolute magnitudes of g_{CD} and g_{CPL} are on the order of 10^{-3}−10^{-5}. Conversely, when highly electric-dipole-forbidden-transitions (*edft*) are present,[19] extremely weak absorption and weak emission intensities are observed, and the absolute magnitudes of g_{CD} and g_{CPL} attain higher values of 10^{-1}−10°. Thus, a contradictory relationship exists for the absolute magnitudes between g_{CD}/g_{CPL} and Φ_{PL} values for isolated, optically active molecules and polymers.

On the basis of the point-dipole approximation,[18−20] the energy spacing of the two split bands $E^{\pm}$ between the degenerate coupled oscillators 1 and 2 with transition dipole moment μ, interdistance r_{12}, and energy E is written as:[19b]

$$E^{\pm} = E \pm \mu^2 \times {r_{12}}^{-3} \times (\sin\alpha \sin\gamma \cos\tau + 2\cos\alpha\cos\gamma)$$

In the case of α = 90° and γ = 90° while τ twisting angle between two chromophores,

$$\Delta E^{\pm} = E^{+} - E^{-} = 2\mu^2 {r_{12}}^{-3} \times \cos\tau \text{ at } E$$

This expression suggests that a subtle change in the r_{12} value can efficiently modulate the degree of exciton coupling.

dx.doi.org/10.1021/ma201665n |*Macromolecules* 2011, 44, 7511–7519

The degenerate coupled oscillator rotational strength is given as:[19b] $R^{\pm} = \pm E\mu^2 r_{12}(4\hbar)^{-1} \times (\sin\alpha \sin\gamma \sin\tau)$.

In the case of $\alpha = 90°$ and $\gamma = 90°$, $R^{\pm} = \pm E\mu^2 r_{12}(4\hbar)^{-1} \times \sin\tau$.

By combining the two equations, one can obtain a simple equation of CD/CPL enhancements: $R^{\pm}/\Delta E^{\pm} = E(8\hbar)^{-1} \times \tan\tau \times {r_{12}}^4 \propto {r_{12}}^4$. This led to an idea that a longer r_{12} value may contribute a significant enhancement in $R^{\pm}$ value, though $\Delta E^{\pm}$ is fairly small, in the case of $\alpha = \gamma = 90°$. As for a longer r_{12} distance of 2 nm, a significant enhancement in $R^{\pm}$ value by 1200 times is in principle possible, compared to a shorter $r_{12} = 0.34$ nm for typical interdistance of $\pi-\pi$ stacks.

Actually, significant enhancement of the observed g_{CD} and g_{CPL} values for the polysilane aggregates originates from long-range order of the chiral aggregates with a longer $r_{12} \sim 2$ nm in a fluid, enabling a collective mode of a weaker coupling between numerous luminous chromophores. A high absorptivity due to *edat* normalized by repeating unit, $\varepsilon \sim 4 \times 10^4$, corresponds to an $\varepsilon \sim 2 \times 10^7$ by the addition of individual polysilanes with DP $\sim$ 500. A huge collective oscillator strength ($f \propto \mu^2$) of $\sim$50 for 500-mer polymers is obtained based on an f of 0.1 for a 10-mer oligosilane.

The primary factor giving the higher Φ_{PL} is the extremely long q values of the present helical rod polysilanes. The highly delocalized exciton state in the long conjugated segment is almost free from intersegment excitation transfer and trapping at the localized sites, hence giving fluorescence with lifetimes identical to the radiative lifetime of the conjugated systems. These characteristics originate from rather the long-q length than intermolecular r_{12} distances in the aggregates.

The characteristics of the aggregates composed of helical rod polysilane chains include (a) significant oscillator coupling of a twist form between chromophoric luminophore rods ($\sim$100 nm in length for $M_w = 8 \times 10^4$) with $\sim$2 nm spacing is possible because the coupling originates from *edat*; (b) the photoexcited energy state due to splitting, $\Delta E^{\pm}$, being as small as $\sim$0.15 eV (1200 cm^{-1}), compared with the first Cotton CD band (E_1) of 3.83 eV (325 nm), yielding a ratio of $\Delta E^{\pm}/E_1 \sim 0.039$ in which the $\Delta E^{\pm}$ value is approximately 6 times that of the thermal energy at $\sim$0.026 eV (300 K); and (c) twisted screw sense being determined by the contact between chiral side chains and/or helical main chains. The smaller $\Delta E^{\pm}$ value in part c in conjunction with a minimal electron−phonon coupling between giant chromophoric luminophores, which are chirally arranged over a distance of $\sim$2 nm, may allow minimal loss of photoexcited energy because a high degree of helicity is retained during the relaxation process of the photoexcited energy. This behavior may be due to an intermediate coupling regime in electronic energy transfer among chromophoric luminophores.[10] Left- and right-CP light generated by incoherent light excitation would travel and circulate through the $\sim$5-μm aggregate and relax to the ground state.

For **1**-*S*, the negative sign of the first Cotton ORD band at 330 nm is consistent with the negative sign of the 330 nm CPL band (Figure 2, parts b and c), and the wavelengths of these two bands (330 nm) are very consistent. An ORD or circular birefringence spectrum can be expressed as $\psi \sim \pi/\lambda\,(n_L - n_R) = c\pi/\lambda\,(1/v_L - 1/v_R)$, where c is the speed of light in a vacuum, λ wavelength in a vacuum, n_L and n_R refractive indices for LCP and RCP light, respectively, and v_L and v_R are speed for LCP and RCP light in the medium, respectively.[14] Hence, the negatively signed ORD signal indicates that $n_R > n_L$ at 330 nm, suggesting that, compared to LCP light, RCP light travels slowly and is effectively confined within the aggregates; conversely, the positively signed, second Cotton ORD signal at 319 nm indicates that $n_L > n_R$, suggesting that LCP light travels slowly compared to RCP light. This situation indicates that a slow light at 330 nm and a slow light at 319 nm for RCP and LCP light, respectively, are possible, implicating that 319 nm LCP light is effectively switched to the 330 nm RCP light, as shown in a modified Jablonski diagram (Figure 7), which is an extension of a classical photoexcitation relaxation scheme with an inversion of CP light screw sense.

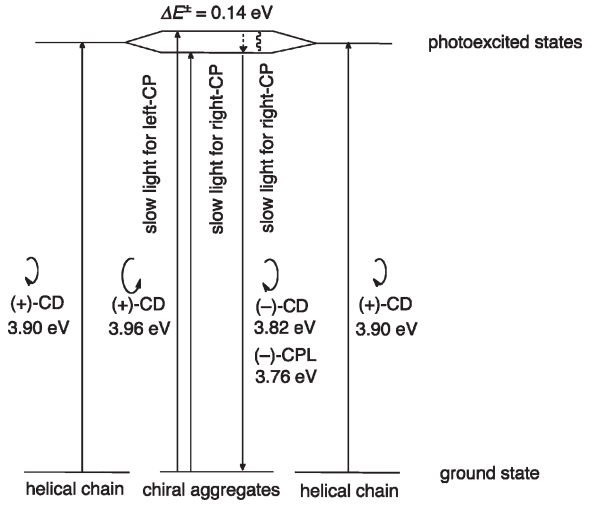

Figure 7. Modified Yablonski diagram of a helical polysilane **1**-*S* and **2**-*S* aggregate (degenerate case) with the preferred CP light in the photoexcited states.

The most striking feature of the aggregates studied in the present report is that the $|g_{CD}|$ value for **1**-*S* aggregates at 25 °C maximizes at a very specific refractive index at the Na-D line (n_D) of the cosolvent (Figure 8, part a) when a series of THF/methanol cosolvents and four other good/poor cosolvents were investigated. The original data are shown in Figures 5a, S4b, and S6(Supporting Information). The degree of optical confinement of the polysilane aggregate in cosolvent is controllable through simple mixing of these good and poor solvents. The role of cosolvent is to act as an organic optofluid to tune the n_D value though an optofluid may be not yet common in polymer science.

According to Psaltis et al.,[13] optofluidics refers to certain optical system made with fluids as a basic component. The fluids are easy to tune optical properties to design unique devices, that cannot be seen in ordinary rigid solid equivalents. Typical features are the abilities of (i) changing the optical property of the fluid medium within a device by simply replacing with another fluid, (ii) providing the optically smooth interface between two immiscible fluids, and (iii) flowing streams of miscible fluids to generate gradients in optical properties by diffusion. Most solid-materials-based optical systems are replaceable with functional fluids with much freedom and flexibility. Typical examples are the oil-immersion microscope, liquid mirrors for telescopes, liquid-core optical fibers, and electrowetting lenses.

The n_D values for polysilane aggregates in good solvents are: 1.44 (chloroform), 1.40 (THF), and 1.50 (toluene); the n_D values for polysilane aggregates in poor solvents are: 1.32 (methanol), 1.36 (ethanol), and 1.34 (acetonitrile). The n_D values of the polysilane aggregates dispersed in cosolvent are assumed to be less than 1.6 because most dialkylpolysilanes have a $n_D \sim 1.62$ in a film state.[21] Although an exact refractive index of polymer aggregate including cosolvents is unclear, the value should be less than that of

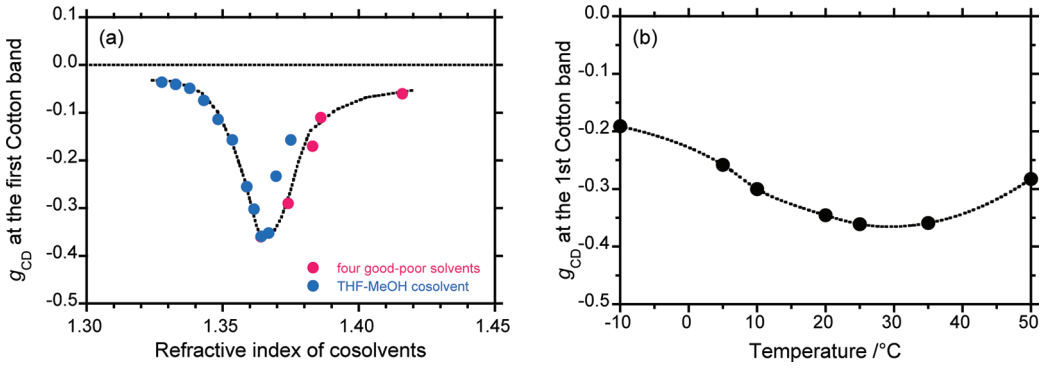

Figure 8. (a) Values of g_{CD} at ~325 nm for **1-*S*** (M_w = 88 500, M_w/M_n = 1.22) in a series of THF/methanol cosolvents and four other good/poor cosolvents (THF/acetonitrile, THF/ethanol, chloroform/methanol, and toluene/methanol) (1.7/1.3 (v/v), 800 rpm (CW) stir rate) at 25.0 °C. [Si repeating unit] = 6.25×10^{-6} mol L^{-1}. (b) Values of g_{CD} at 325 nm for **1-*S*** in THF/methanol (1.7/1.3 (v/v), 800 rpm (CW) stir rate) as a function of temperature.

the film. By an analogy with the technology of optical fibers composing of a higher refractive index core and a lower refractive index clad, a relative refractive index of the aggregate to the cosolvent is crucial to control numerical aperture, leading to an efficiently confinement of LCP and RCP light at different wavelengths in the aggregate.

The g_{CD} value at 325 nm for **1-*S*** aggregates in THF/methanol = 1.7/1.3 (v/v) is plotted as a function of solution temperature in Figures 8b and S4a (Supporting Information). The $|g_{CD}|$ values exhibited a maximum at 25−35 °C and decreased above and below this temperature range. The **1-*S*** aggregates dispersed in the cosolvent can self-regulate when subjected to changes in temperature. The self-tuning of the refractive index of the aggregates in the cosolvent results in the efficient generation of one-handed CP-light under *unpolarized* light excitation.

The M_w of the polysilanes is another critical factor that can enhance the $|g_{CD}|$ and $|g_{CPL}|$ value because there is a maximum M_w value that closely corresponds to the q value characteristic of the chain-like polymer. In Figure 2d taken from Figure S2 (Supporting Information), the g_{CPL} and g_{CD} values for the **1-*S*** aggregates are shown as a function of M_w (11 000 ≤ M_w ≤ 2 160 000) along with the corresponding CD/UV/CPL/PL spectra (Figure 2a−c). On the basis of these experiments, **1-*S*** with a M_w of 88 500 was found to produce the maximum absolute values, suggesting that an ideal molecular weight will yield the largest CD and CPL amplitudes. This specific M_w value is comparable to the q value inherent to the **1-*S*** polysilane, which is able to adopt an ideal rod structure in fluid solution at ambient temperature. Similarly, **2-*S*** and **2-*R*** exhibited maximum g_{CD} and g_{CPL} values at a specific M_w value among three different tested M_ws (Figures 6 and S3 (Supporting Information)). Among the three M_ws, the M_w values of ~4 540 000, 108 000, and 25 200 for **2-*S*** and ~6 100 000, 80 900, and 9060 for **2-*R*** are comparable to the q values inherent to **2-*S*** and **2-*R***, which are somewhat shorter that the q-value of **1-*S***.

On the basis of membrane filtration experiments using a series of different pore sizes (1, 3, 5, and 10 μm filters; Millipore), the aggregate size of **1-*S*** did not affect the g_{CD} value (Figure 3b); however, the absorbance and CD signals both decreased dramatically when smaller pore sizes were used (Figure 3a and S1 (Supporting Information)). Thus, the observed CD signal amplitudes are determined predominantly by the exciton coupling of the nearest neighbor polysilanes in the aggregates.

The g_{CD} values for **1-*S*** aggregates did not exhibit a vortex effect in THF/methanol solution under clockwise (CW) or counterclockwise (CCW) stirring at four different stirring speeds (0, 400, 800, and 1300 rpm) (Figure S7, Supporting Information). The vortex-induced Cotton CD effect generated by mechanically stirring a fluid in a cuvette was recently reported to provide CD and linear dichroism (LD) spectra that dynamically reflect locally different fluidic situations in several supramolecular systems,[22] including a rod-shaped supramolecular polymer made of zinc porphyrins bearing pyridyl and two carboxylic acid groups. These effects were due to a temporal alignment of the nanofibers along the chiral fluidic flows. However, the optical activity of **1-*S*** was unchanged even in fluidic conditions. Figure S8 (Supporting Information) shows changes in CD/UV spectra of the g_{CD} value at 325 nm for the **1-*S*** aggregates at three M_ws in THF/methanol = 1.7/1.3 (v/v) as a function of time. Optically active **1-*S*** aggregates at higher M_ws were very stable because these g_{CD} values were very weakly dependent on time.

Recently, the efficient generation of RCP or LCP light from artificial systems has received significant attention due to unique CP-origin applications, including laser, light-emitting diode, optical filter, and optical information storage. On the basis of to this goal, luminophore-doped liquid crystals,[23,24] chiral π-conjugated polymer films,[25,26] sculptured structures by glancing angle deposition,[27] optical confinement in a vertical cavity chiral surface,[28] and planar-type chiral nanostructural surfaces[29] have been employed. Although luminescent rare-earth metal ions with chiral organic ligands, which exhibit high g_{CPL} values of up to ~1.4,[30] may be another class of candidates, Φ_{PL} was limited to less than 2% due to *edft* origin.

Our solution-processed, optically active luminescent aggregates in an organic optofluids may possess considerable advantages because various solvents, including achiral solvents and/or chiral terpenes (limonenes, pinenes, and carvone), can freely mix together, allowing for fine-tuning and optimization of the optical activity while retaining the inherently high Φ_{PL}. The product yield is near 100% due to the lossless precipitation method under mild conditions at ambient temperature in only a few minutes. These aggregates are promising as chiroptical inks for CP-related device applications,[31] if the aggregate dispersed into amorphous polymer film and gel-like matrices as plastic optofluids with a tuned refractive index were employed in place of tuned liquid optofluid. Alternatively, the present demonstration of an absolutely artificial, optically active aggregate in an optofluid system may provide new insight for efficient light-harvesting and charge-separation

mechanisms in photosynthetic biosystems under incoherent *unpolarized* sunlight.[1,2]

CONCLUSION

Under optimized conditions (molecular weight, a relative ratio of good-and-poor solvents, and temperature), **1-*S*** aggregates with ~5 μm in the suspension of organic fluid solvents efficiently generated CPL with $g_{CPL} = -0.7$ at 330 nm with an *fwhm* of 0.18 eV (1450 cm^{-1}) while retaining a high quantum efficiency ~53% at room temperature upon incoherent unpolarized photoexcitation at 290 nm. This intense g_{CPL} value results from the intense bisignate CD signals ($g_{CD} = -0.35$ at 325 nm and +0.31 at 313 nm), arising from collective coupled oscillators with *edat* origins. Also, **2-*S*** and **2-*R*** aggregates provided similar intense CD and CPL spectra. The most critical factors for these enhanced CD/CPL amplitudes of the polysilane aggregates were the backbone configuration and molecular weight of **1-*S***, **2-*S***, and **2-*R*** and a refractive index of good/poor cosolvents as organic fluid.

The former is connected to the chain stiffness of rod-like helical polysilanes. A longer interchain distance of **1-*S***, **2-*S***, and **2-*R*** aggregates dispersed in solution was assumed to be responsible for a significant enhancement in CD and CPL by three order of the magnitude, compared to isolated polysilane chains dissolved in an isotropic solution.

The latter may be due to an efficient confinement effect of CP-light in the chiral aggregate dispersion from incoherent unpolarized UV light. The most essential role of the organic fluid is to act as an optofluid to efficiently tune the relative refractive index between the fluid and the aggregates. The optically tuned fluid is capable of slow-light CP light enhancement of the chiral aggregate as dispersion medium under incoherent unpolarized UV light excitation.

EXPERIMENTAL SECTION

Materials. The highly emissive helical luminophores poly[*n*-decyl-(*S*)-2-methylbutylsilane] (**1-*S***), poly[*n*-dodecyl-(*S*)-2-methylbutylsilane] (**2-*S***), and poly[*n*-dodecyl-(*R*)-2-methyl- butylsilane] (**2-*R***), were synthesized via Wurtz condensation of the corresponding organodichlorosilane with sodium in hot toluene in the presence of 2 mol % of 18-crown-6-ether (Scheme S1, Supporting Information).[3,4] A typical procedure for the production of **1-*S*** aggregates in a mixture of THF and methanol is described. First, 1.3 mL of methanol was added in one bolus to 1.7 mL of a THF solution containing polysilane (6.25×10^{-6} M as a repeating unit) in a synthetic quartz cuvette, which was placed in the Peltier apparatus of a JASCO J820 spectropolarimeter at 25 °C and stirred for 10 s. After the addition of 1.3 mL of methanol at 25 °C to the solution, a slightly white turbid solution of polysilane aggregates dispersed in the mixed solvent was instantly formed. After stirring for 10−30 s, this solution was used for the CD/UV, ORD/UV, and CPL/PL studies. Other polysilane aggregates were obtained using a similar process. The size of **1-*S*** particles ranged from 1−10 μm, as measured by evaluating the changes in CD/UV signal intensities after filtering the solution with PTFE membrane filters with different pore sizes (1/3/5/10-μm) (Millipore).[32]

Chiroptical Analysis. As a measure of the degree of CPL,[19] the dimensionless parameter g_{CPL} is defined as $2(I_L - I_R)/(I_L + I_R)$, where I_L and I_R refer to left- and right-handed luminescence intensity, respectively, arising from unpolarized excitation. Similarly, the dimensionless parameter[19] g_{CD} is defined as $2(\varepsilon_L - \varepsilon_R)/(\varepsilon_L + \varepsilon_R)$, where ε_L and ε_R refer to left- and right-handed absorptivity per repeating unit, respectively. The values of $|g_{CPL}| = 2$ and $|g_{CD}| = 2$ refer to pure, single-handed circularly polarized light at the excited and ground states; thus, the experimental values of g_{CPL} and g_{CD} become a measure of chirality at the excited and ground states, respectively.

ASSOCIATED CONTENT

Supporting Information. Preparation scheme of polysilanes, table of Cotton bands and Stokes shifts, and figures showing CD and UV spectra of **1-*S***, **2-*S***, and **2-*R*** aggregates in various good solvent/poor solvent ratios, with/without various membrane filters, various molecular weights, clockwise and counterclockwise stirring operation with different speeds, and solution temperature. This material is available free of charge via the Internet at http://pubs.acs.org.

AUTHOR INFORMATION

Corresponding Author

*Telephone: +81-743-726040. Fax: +81-743-726049. E-mail: fujikim@ms.naist.jp.

Present Addresses

[§]Institute for Complex Molecular Systems, Department of Biomedical Engineering, Department of Chemical Engineering and Chemistry, Eindhoven University of Technology, P.O. Box 513, 5600 MB Eindhoven, The Netherlands. E-mail: Y.Nakano@tue.nl.

ACKNOWLEDGMENT

The authors are grateful for financial supports from a Grant-in-Aid for Scientific Research (B) (22350052, FY2010−FY2014) from the Ministry of Education, Culture, Sports, Science and Technology, Japan and the Sekisui Chemical Grant Program for Research on Manufacturing Based on Learning from Nature (FY2010). We thank Profs. Hiroshi Masuhara, Teruki Sugiyama, Hisao Yanagi, Yasuchika Hasegawa, Atsushi Ikeda, Kotohiro Nomura, and Takahiro Sato for inspiring discussions and Yasuo Okajima for assisting with PL decay experiments. We also thank Fumiko Ichiyanagi and Prof. Yongyang Yang for fruitful discussions and preliminary work. The work is dedicated to the late Prof. Akio Teramoto (Osaka University, Emeritus).

REFERENCES

(1) For an early review, see: Steinberg, I. Z. *Annu. Rev. Biophys. Bioeng.* **1978**, *7*, 113–137.

(2) (a) Barzda, V.; Musthrdy, L.; Garab, G. *Biochemistry* **1994**, *33*, 10837–10841. (b) Barzda, V.; Istokovics, A.; Simidjiev, I.; Garab, G. *Biochemistry* **1996**, *35*, 8981–8985. (c) Gussakovsky, E. E.; Shahak, Y.; van Amerongen, H.; Barzda, V. *Photosynth. Res.* **2000**, *65*, 83–92.

(3) (a) Fujiki, M. *J. Am. Chem. Soc.* **1994**, *116*, 6017–6018. (b) Fujiki, M. *Appl. Phys. Lett.* **1994**, *65*, 3251–3253. (c) Fujiki, M. *Symmetry* **2010**, *2*, 1625–1652.

(4) For a review, see: (a) Fujiki, M.; Koe, J. R.; Terao, K.; Sato, T.; Teramoto, A.; Watanabe, J. *Polym. J.* **2003**, *35*, 297–344. (b) Fujiki, M. *Chem. Rec.* **2009**, *9*, 271–298.

(5) (a) Kawagoe, Y.; Fujiki, M.; Nakano, Y. *New J. Chem.* **2010**, *34*, 637–647. (b) Nakano, Y.; Liu, Y.; Fujiki, M. *Polym. Chem.* **2010**, *1*, 460–469. (c) Zhang, W.; Yoshida, K.; Fujiki, M.; Zhu., X. *Macromolecules* **2011**, *44*, 5105–5111.

(6) (a) Lakowicz, J. R. *Principles of Fluorescence Spectroscopy*, 3rd ed.; Springer: Heidelberg, Germany, 2006. (b) Birks, J. B. *Photophysics of Aromatic Molecules*; Wiley: London, 1970. (c) Malkin, J. *Photophysical and Photochemical Properties of Aromatic Compounds*; CRC: Boca Raton,

FL, 1992. (d) Turro, N. J. *Modern Molecular Photochemistry*; University Science Books: Mill Valley, CA, 1991.
(7) For a recent review, see: Hong, Y.; Lam, J. W. Y.; Tang, B. Z. *Chem. Commun.* **2009**, 4332–4353.
(8) Collini, E.; Wong, C. Y.; Wilk, K. E.; Curmi, P. M. G.; Brumer, P.; Scholes, G. D. *Nature (London, U.K.)* **2010**, *463*, 644–648.
(9) Engel, G. S.; Calhoun, T. R.; Read, E. L.; Ahn, T.-K.; Mancăl, T.; Cheng, Y.-C.; Blankenship, R. E.; Fleming, G. R. *Nature (London, U.K.)* **2007**, *446*, 782–786.
(10) Collini, E.; Scholes, G. D. *J. Phys. Chem. A* **2009**, *113*, 4223–4241.
(11) Scholes, G. D. *J. Phys. Chem. Lett.* **2010**, *1*, 2–8.
(12) (a) Sherwin, J. A.; Lakhtakia, A. *Opt. Commun.* **2002**, *214*, 231–245. (b) Pedersen, J.; Mortensen, N. A. *Appl. Phys. Lett.* **2007**, *91*, 213501. (c) Mortensen, N. A.; Xiao, S. *Appl. Phys. Lett.* **2007**, *90*, 141108. (d) Arango, F. B.; Christiansen, M. B.; Gersborg-Hansen, M.; Kristensen, A. *Appl. Phys. Lett.* **2007**, *91*, 223503. (e) For a review, see: Hunt, H. C.; Wilkinson, J. S. *Microfluid Nanofluid* **2008**, *4*, 53–79.
(13) Psaltis, D.; Quake, S. R.; Yang, C. *Nature (London, U.K.)* **2006**, *442*, 381–386.
(14) Charney, E. *The Molecular Basis of Optical Activity — Optical Rotatory Dispersion and Circular Dichroism*; Wiley: New York, 1979.
(15) For reviews, see. (a) Teramoto, A. *Prog. Polym. Sci.* **2001**, *26*, 667–720. (b) Sato, T.; Terao, K.; Teramoto, A.; Fujiki, M. *Polymer* **2003**, *44*, 5477–5495.
(16) (a) Watanabe, J.; Kamee, H.; Fujiki, M. *Polym. J.* **2001**, *33*, 495–497. (b) Okoshi, K.; Kamee, H.; Suzaki, G.; Tokita, M.; Fujiki, M.; Watanabe, J. *Macromolecules* **2002**, *35*, 4556–4559.
(17) For a review, see: Miller, R. D.; Michl, M. *Chem. Rev.* **1989**, *89*, 1359–1410.
(18) Berova, N. *Chirality* **1997**, *9*, 395–406.
(19) (a) Dekkers, H. P. J. M. In *Circular Dichroism: Principles and Applications*, 2nd ed.; Chapter 7, Berova, N., Nakanishi, K., Woody, R. W., Eds.; Wiley−VCH: New York, 2000. (b) Rodger, A.; Nordén, *Circular Dichroism and Linear Dichroism*; Oxford University Press: Oxford, U.K., 1997.
(20) Langeveld-Voss, B. M. W.; Beljonne, D.; Shuai, Z.; Janssen, R. A. J.; Meskers, S. C.; Meijer, E. W.; Brédas, J.-L. *Adv. Mater.* **1998**, *10*, 1343–1348.
(21) Sato, T.; Nagayama, N.; Yokoyama, M. *J. Mater. Chem.* **2004**, *14*, 287–289.
(22) (a) Ribó, J. M.; Crusats, J.; Sagués, F.; Claret, J.; Rubires, R. *Science (Washington, DC)* **2001**, *292*, 2063–2066. (b) Tsuda, A.; Alam, M. A.; Harada, T.; Yamaguchi, T.; Ishii, N.; Aida, T. *Angew. Chem., Int. Ed.* **2007**, *46*, 8198–8202. (c) Wolfs, M.; George, S. J.; Tomovic, Z.; Meskers, S. C. J.; Schenning, A. P. H. J.; Meijer, E. W. *Angew. Chem., Int. Ed.* **2007**, *46*, 8203–8205.
(23) Chen, S. H.; Katsis, D.; Schmid, A. W.; Mastrangelo, J. C.; Tsutsui, T.; Blanton, T. N. *Nature (London, U.K.)* **1999**, *397*, 506–508.
(24) Furumi, S.; Sakka, Y. *Adv. Mater.* **2006**, *18*, 775–780.
(25) (a) Oda, M.; Notheofer, H.-G.; Lieser, G.; Scherf, U.; Meskers, S. C. J.; Neher, D. *Adv. Mater.* **2000**, *12*, 362–365. (b) Wilson, J. N.; Steffen, W.; McKenzie, T. G.; Lieser, G.; Oda, M.; Neher, D.; Bunz, U. H. F. *J. Am. Chem. Soc.* **2002**, *124*, 6830–6831. (c) Tang, H.-Z.; Fujiki, M.; Motonaga, M. *Polymer* **2002**, *43*, 6213–6220. (d) Yorozuya, S.; Osaka, I.; Nakamura, A.; Inoue, Y.; Akagi, K. *Synth. Met.* **2003**, *135*, 93–94.
(26) Yu, J.-M.; Sakamoto, T.; Watanabe, K.; Furumi, S.; Tamaoki, N.; Chen, Y.; Nakano, T. *Chem. Commun.* **2011**, *47*, 3799–3801.
(27) Krause, K. M.; Brett, M. J. *Adv. Funct. Mater.* **2008**, *18*, 3111–3118.
(28) Iba, S.; Koh, S.; Ikeda, K.; Kawaguchi, H. *Appl. Phys. Lett.* **2011**, *98*, 081113.
(29) (a) Volkov, S. N.; Dolgaleva, K.; Boyd, R. W.; Jefimovs, K.; Turunen, J.; Svirko, Y.; Canfield, B. K.; Kauranen, M. *Phys. Rev. A* **2009**, *79*, 043819. (b) Tzuang, L. D.-C.; Jiang, Y.-W.; Ye, Y.-H.; Chang, Y.-T.; Wu, Y.-T.; Lee, S.-C. *Appl. Phys. Lett.* **2009**, *94*, 091912. (c) Konishi, K.; Nomura, M.; Kumagai, N.; Iwamoto, S.; Arakawa, Y.; Kuwata-Gonokami, M. *Phys. Rev. Lett.* **2011**, *106*, 057402.
(30) (a) Lunkley, J. L.; Shirotani, D.; Yamanari, K.; Kaizaki, S.; Muller, G. *J. Am. Chem. Soc.* **2008**, *130*, 13814–13815. (b) Harada, T.; Nakano, Y.; Fujiki, M.; Naito, M.; Kawai, T.; Hasegawa, Y. *Inorg. Chem.* **2009**, *48*, 11242–11250.
(31) (a) Ono, H.; Takahashi, F.; Emoto, A.; Kawatsuki, N. *J. Appl. Phys.* **2005**, *97*, 053508. (b) Stanciu, C. D.; Hansteen, F.; Kimel, A. V.; Kirilyuk, A.; Tsukamoto, A.; Itoh, A.; Rasing, Th. *Phys. Rev. Lett.* **2007**, *99*, 047601. (c) Nakagawa, K.; Ashizawa, Y.; Ohnuki, S.; Itoh, A.; Tsukamoto, A. *J. Appl. Phys.* **2011**, *109*, 07B735.
(32) We characterized the aggregate size by a series of membrane filters with several pore sizes, although the dynamic light scattering (DLS) technique (Otsuka DLS-6000, Japan) might provide straightforward information of the size and its distribution of the aggregates. We applied this technique to evaluate approximately micrometer-order aggregates but failed due to being out of range of the instrument (up to 1 μm).